Korean J. Chem. Eng., 40(11), 2646-2656 (2023)
DOI: 10.1007/s11814-023-1472-5

pISSN: 0256-1115
eISSN: 1975-7220

Electrocatalytic reduction of furfural for selective preparation of 2-methylfuran over a sandwich-structured Ni-Cu bimetallic catalyst

Yiming Cui*,, Ze Wang*,**,†, and Songgeng Li*,****

*State Key Laboratory of Multi-Phase Complex Systems, Institute of Process Engineering, Chinese Academy of Sciences, Beijing 100190, China
**Sino-Danish College, University of Chinese Academy of Sciences/Sino-Danish Center for Education and Research, Beijing 100190, China
(*Received 5 December 2022 • Revised 28 March 2023 • Accepted 10 April 2023*)

Abstract−The electrocatalytic reduction (ECR) of furfural (FF) for synthesis of 2-methylfuran (MF) is investigated, using a sandwich-structured electrode (NiCu/CalZIF/CP), with an inner substrate of carbon paper (CP), a surface layer of Ni-Cu bimetallic catalyst (metal layer), and a middle layer of calcined Ni-ZIF-8 (CalZIF) particles. It is found that the production rate (PR) and Faradaic efficiency (FE) of MF increase with the increase of metal loading, while the variation becomes stable in higher dosages. The FE of MF illustrates a rising-first-and-declining-later trend with the increase of current density, but in a slight degree compared with the system without CalZIF, indicating a better stability on anti-interference of current. The PR of MF increases with increasing current first and then becomes stable, which differs to the reducing trend in higher currents in the system without CalZIF. Under the optimized conditions with H_2SO_4 concentration of 0.2 M and current density of 12 $mA \cdot cm^{-2}$, the total FE of organics, the FE of MF, and the PR of MF, respectively reach to their maximum values of 82%, 66% and 75 $\mu mol \cdot cm^{-2} \cdot h^{-1}$, under the catalytic effects of the composite electrode with optimal Ni/Cu ratio of 0.04, metal layer loading amount of 3 $mg \cdot cm^{-2}$, and CalZIF dosage of 1 $mg \cdot cm^{-2}$. The electrode can be regenerated after re-elctrodeposition treatment. The deactivation of catalyst is found relative to the loss and agglomeration of the metals, which is resulted from the corrosion and rearrangement of the metal atoms over the electrode surface.

Keywords: Furfural, Hydrodeoxygenation, Electrocatalytic Reduction, 2-Methylfuran, Mechanism

INTRODUCTION

2-Methylfuran (MF) can widely be used for producing pesticides, perfumes, drugs [1,2], and fuel additives with high octane number (103) and adequate energy density (28.5 $MJ \cdot L^{-1}$) [3,4]. It is usually produced from hydrodeoxygenation of furfural (FF) in H_2 atmosphere, under a high temperature and high pressure condition, leading to a severe risk of security.

Recently, the electrocatalytic reduction (ECR) method has been widely studied in many fields including the electrolysis of water to produce H_2 particularly with some non-noble metal catalysts [5-8], the reduction of CO_2 to produce CO, CH_4, methanol, formate and C2 compounds [9-11], the reduction of N_2 to synthesize ammonia [12,13], the upgrading of model components in bio-oil [14-16], and etc. FF is also a typical component in bio-oil, and the ECR of FF to produce MF through hydrodeoxygenation has aroused great interest as well, because of many aspects of advantages [17, 18]. For instance, the reaction condition is mild (usually under atmosphere pressure at room temperature), the electricity used in the system can be obtained from the renewable solar or wind power, and no external H_2 is needed since H_2 can be in-situ produced from electrolysis of water [19-22].

In the reaction system for ECR of FF, there are mainly three half-cell reactions in cathode zone, respectively with the generations of MF, furfuryl alcohol (FA) and H_2. Among them, the formations of MF and FA are products from ECR of FF, and MF is the aim product herein. The formation of H_2 by hydrogen evolution reaction (HER) is a main side reaction, as it consumes electrons and lowers the Faradaic efficiency (FE) for ECR of FF. Another side reaction is the dimerization of two alcohol radicals (·C-OH) through direct electroreduction, and the product is hydrofuroin (HF). The reactions are illustrated in Eqs. (1)-(4).

$$FF + 4H^+ + 4e^- \rightarrow MF \quad (1)$$

$$FF + 2H^+ + 2e^- \rightarrow FA \quad (2)$$

$$2H^+ + 2e^- \rightarrow H_2 \quad (3)$$

$$2FF + 2H^+ + 2e^- \rightarrow HF \quad (4)$$

Usually, an electrode with low hydrogen overpotential (e.g., platinum-group metals) is favorable for the mechanism of ECR; on the contrary, the electroreduction mechanism is more preferred on an electrode with high hydrogen overpotential (e.g., Pb, Hg, Cd, and graphite); the two reactions may happen simultaneously on an electrode with intermediate hydrogen overpotential (e.g., Ni, Co, Fe, Cu, Ag and Au) [2].

†To whom correspondence should be addressed.
E-mail: wangze@ipe.ac.cn

Nilges and Schröder [23] reported that Cu was the best electrode for producing MF from ECR of FF; furfuryl alcohol (FA) was the primary product over the electrode of Pt; generally equal amounts of FA and MF were produced on Ni electrode; the dimer product from pinacol coupling reaction was the most prominent product over the electrodes of Al, Pb, Fe, and C, while nearly no dimers were detected on Pt or Cu.

May and Briddinger [24] generalized that for the ECR of FF over Cu electrode, the initial concentration of FF was suggested to be 20-100 mM to yield more FA or MF, because a high concentration of FF might lead to the generation of humins, while a low concentration of FF favored the formation of H_2. An aqueous-organic cosolvent such as acetonitrile in water with a ratio of 20%-80% at a low pH value less than 2 was preferable for producing MF. A lower potential less than −800 mV vs RHE (reversible hydrogen electrode) was preferred to avoid significant formation of H_2.

Chadderdon et al. [25] investigated the ECR of FF in an acidic electrolyte on Cu electrode. The results showed that the reactions of ECR and electroreduction can both happen under the catalysis of Cu, leading to the formations of FA, MF, and the dimer product of HF. FA and HF were more produced in an electrolyte with high pH value, while a low-pH electrolyte favored the generation of MF and H_2. A low initial concentration of FF was strongly beneficial to the formation of H_2, while a high value favored the generation of FA, and a high selectivity of MF could be achieved under a medium initial concentration of FF.

The types of Cu material and the modification of Cu electrode were also investigated. Biddinger et al. [21] found that Cu nanocrystals were more reactive and stable than microcrystals or plates of Cu. Zhou et al. [17] found that the selectivity of MF and the efficiency of current could both be improved when a small amount of Pd was mixed with Cu. In Dixit et al.'s work [26], a porous bimetallic Ni-Cu catalyst over a high-surface-area Ni-foam was tested for ECR of FF in alkaline electrolyte, while the products of FA and HF instead of MF were high efficiently obtained.

At present, the FE and the PR of MF are generally in lower levels, so intensive and extensive studies are still necessary and quite important. In this work, the preparation of MF from ECR of FF was investigated with a supported Ni-Cu bimetallic catalyst. Based on the prepared Ni-Cu catalyst, the influence of the loading amount of metals, the electrolyte acidity and the current density were studied to maximize the production of MF. Particularly, as an innovative idea, a sandwich like electrode (NiCu/CalZIF/CP), with an inner substrate of carbon paper (CP), a surface layer of Ni-Cu bimetallic catalyst (metal layer), and a middle layer of calcined Ni-ZIF-8 (CalZIF) particles, a type of MOF (metal-organic framework) material, is designed to enhance the formation of MF.

MATERIAL AND METHODS

1. Definition of Special Terms

The production rate (PR), carbon balance (CB), current density (CD), and Faradaic efficiency (FE) are calculated as follows:

$$PR=n_p/(t\times A_{cat}) \quad (5)$$

$$CB=(n_{FF}+n_{FA}+n_{MF})/n_{FF,i}\times 100\% \quad (6)$$

$$CD=I/A_{cat} \quad (7)$$

$$FE_p=(z_p\times n_p\times F)/(I\times t)\times 100\% \quad (8)$$

Where, PR indicates the production rate of a product, μmol·$cm^{-2}\cdot h^{-1}$; n_p is the molar amount of the product, μmol; t is the time of reaction, hour for PR and second for FE; A_{cat} is the area of cathode immersed in electrolyte (1.5 cm^2). $n_{FF,i}$ represents the carbon amount of FF added into the electrolyte, mol; n_{FF}, n_{FA}, and n_{MF} indicate the carbon amount of FA, MF and the remained FF after reaction, mol. CD indicates the value of current density, A·cm^{-2}; I is the current powered by the direct-current power, A; FE_p indicates the value of Faradaic efficiency of a product; z_p is the number of electron needed for generation of 1 molecule of product from 1 molecule of FF (4 for MF; 2 for FA); n_p is the molar amount of product, mol; F is the Faraday constant, 96,485 C·mol^{-1}; I is the current supplied by the direct-current power, A.

2. Preparation of Catalyst

The Ni-Cu bimetallic catalyst was prepared by electrodeposition (ED) method on the substrate of carbon paper (CP) with or without a coating layer of CalZIF.

Pretreatment of CP: The CP was firstly degreased by ultrasonic treatment in ethanol for 20 min, followed by 3 times of rinsing with deionized water, and then dried in air for at least 6 hours.

Preparation of Ni-ZIF-8: The Ni-ZIF-8 was synthesized according to the method introduced in Lan et al's work [27]. Firstly, 1.4275 g $Zn(NO_3)_2\cdot 6H_2O$ and 0.5972 g $Ni(NO_3)_2\cdot 6H_2O$ were dissolved in 40 ml methanol, followed by 10 min ultrasonic treatment, giving a solution named as solution-A. Thereafter, 3.1526 g 2-methyl imidazole (2-MeIM) was added into another 40 mL methanol, and then 175 μL solution-A was further added to generate crystal nucleus, followed by ultrasonic treatment for 10 min, giving a solution in the name of solution-B. Subsequently, the two solutions were mixed and treated with ultrasonic wave for 10 min, and then the solution is kept at room temperature for 24 hours without stirring, to grow MOF crystal. The precipitated Ni-ZIF-8 was finally obtained after 3 times of washing and centrifuging with methanol, and dried at 60 °C for 8 h.

Calcination of Ni-ZIF-8: The prepared Ni-ZIF-8 was further calcined (named as CalZIF) in a tube furnace to produce a carbonated material with a structure composed of single atomic Ni surrounded with N atoms. The calcination was conducted in nitrogen atmosphere (20 ml·min^{-1}) under a varied temperature: heated from room temperature (residence for 30 min) to 900 °C (for 2 h) by 5 °C·min^{-1}, and finally cooled in the oven naturally. The general process for preparation of CalZIF is shown in Scheme 1.

Coating CP with CalZIF: The prepared CalZIF powders (20 mg) was dispersed in a solution (1 mL), which is composed of water (0.8 mL), isopropyl alcohol (0.15 mL), and a resin solution of D-520 (0.05 mL, DuPont). Subsequently, the mixture was treated by ultrasonic wave for at least 10 min to get a uniform slurry. Then, 0.075 mL of the slurry (containing 1.5 mg powders of CalZIF) was dropped onto the substrate of CP, and dried at 60 °C for 6 h.

Preparation of the Ni-Cu bimetallic electrode by ED method: The ED reaction was conducted in an undivided electrolytic cell (100 mL). A piece of CP with or without the coating layer of CalZIF (immersed area in electrolyte of 1×1.5 cm^2) was used as the cath-

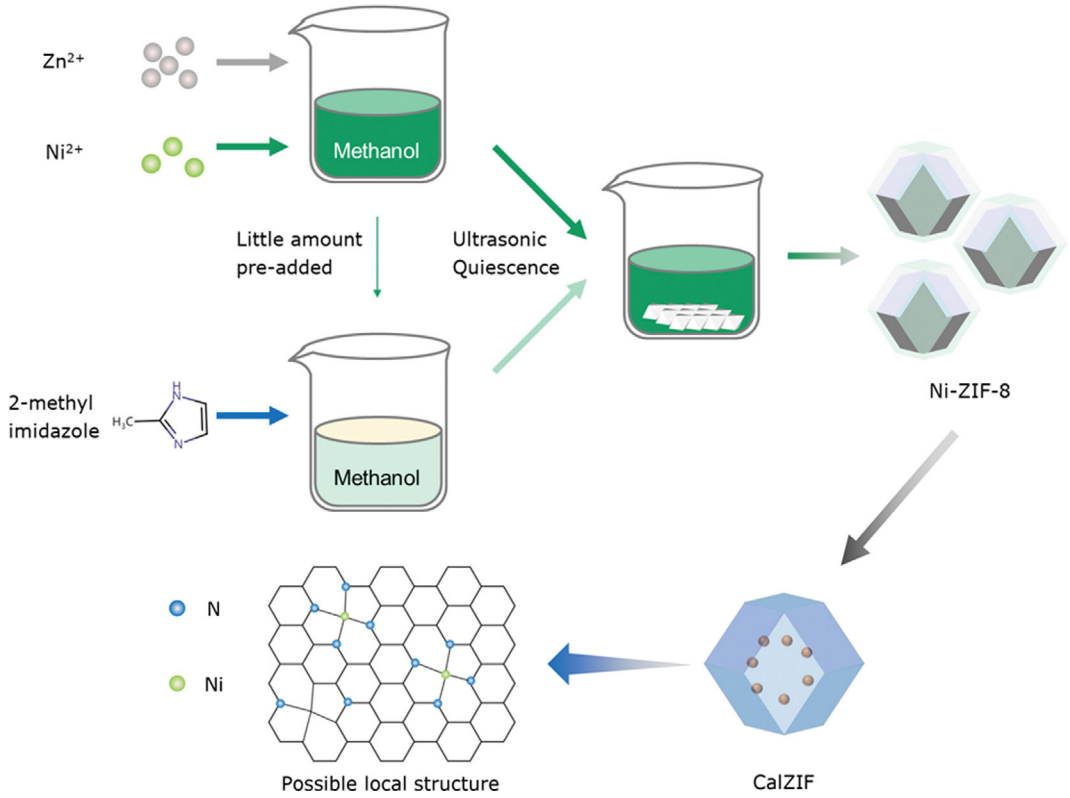

Scheme 1. Process for preparation of CalZIF.

ode, a KCl-saturated Ag/AgCl electrode was used for reference, and a sacrifice Cu electrode was used as the counter electrode. In each run of ED process, a mixture solution of 0.5 M $NiSO_4$, 0.04 M $CuSO_4$ and 0.5 M H_3BO_3 was used as the electrolyte (H_3BO_3 played a buffer role to keep the pH stable at 4.8). The solution was stirred at room temperature using a magnetic stirrer, and the current was supplied with a direct-current power (LPD305C, Lodestar). The loading amount of Ni and Cu is controlled by adjusting the working potential, as the standard electric potential of Ni^{2+}/Ni^0 (−0.257 V) and Cu^{2+}/Cu (0.342 V) are different, and a lower working potential (a high potential absolute value) favors the deposition of Ni^{2+} more than that of Cu^{2+}. Because the ED process is conducted in a constant-current mode, the working potential is adjusted by stirring rate, under the conditions with a current density of 13.3 mA·cm^{-2}, a reaction time of 600 s, and a total charge of 12 C (corresponding to the metal layer amount of 3 mg·cm^{-2}). The conditions are applied to all ED processes if not otherwise specified. The obtained Ni-Cu bimetallic catalysts with and without the mid-layer of CalZIF were respectively named as NiCu/CalZIF/CP and NiCu/CP. The recorded potential was converted into the value against RHE through Eq. (9)

$$E(RHE)=E(Ag/AgCl)+0.0592pH+0.1989V \quad (9)$$

Repetitive results and carbon balance: Repetitive results showed that the relative deviations of the FE of MF and the PR of MF were no higher than 8%, indicating a qualified reliability of the experimental system. The CB values of all experiments are higher than 76%, indicating that FA and MF are two of the major products and some undetectable organics like humins are much less.

3. ECR Reaction

The preparation of MF from ECR of FF was conducted in an H-type cell, which is composed of an anode chamber and a cathode chamber (50 mL for each), separated by a proton exchange membrane. The prior prepared electrode (NiCu/CalZIF/CP or NiCu/CP), a Pt wire, and a KCl-saturated Ag/AgCl electrode, were respectively used as the cathode, the anode, and the reference electrode. Before experiment, 40 ml electrolyte was added into each of the chambers. The cathode electrolyte was composed of FF (40 mM), ethanol (20% volume fraction), water (80% volume fraction), Na_2SO_4 (0.2 M), and H_2SO_4 (0.1-0.6 M). The anode electrolyte has a same composition as the cathode except for the absence of FF. The addition of ethanol was to improve the solubility of organic compounds in the electrolyte. In each run of reaction, the experiment was conducted in a constant-current mode (6-14 mA·cm^{-2}), under normal pressure at 25 °C for 2 hours. If not otherwise specified, the conditions were applied to all ECR experiments.

4. Product Analysis

After reaction, a fraction of the liquid was mixed with the solvent of ethyl acetate (EA), for extraction of organics from water phase. The detailed process was as follows: 0.4 mL electrolyte sample was mixed with 0.6 mL EA in a test tube, followed by agitation using a vortex shaker for 1 min; thereafter, the 0.4 mL organic phase was separated and mixed with 0.4 mL saturated NaCl solution to remove water soluble residue in the organic phase, followed by agitation with the vortex shaker for 1 min. A fraction (0.2 mL) of the organic phase was mixed with a DMF (N, N-Dimethylformamide) solu-

tion (0.2 mL), containing 0.023 M cyclohexanol as the internal standard substance. The final EA-DMF solution was then analyzed with GC/MS (gas chromatography/mass spectrometer) for quantification of products.

The instrument of GC/MS (QP-2020, SHIMADZU) equipped with a DB-FFAP column (30 m-0.25 mm-0.25 μm) and an EI ion source (70 eV) was used for analysis of the EA-DMF solution. The temperature of the GC oven started at 40 °C (5 min), and then increased to 100 °C by 5 °C·min^{-1} (3 min), and finally to 240 °C (1 min) by 5 °C·min^{-1}. The temperature of the inject port, the temperature of the transfer line between GC and MS, and the temperature of the ion source were respectively set at 240 °C, 240 °C, and 200 °C. Both of full scan and single ion monitoring modes were used for identification and quantification of products (searching in NIST-2014).

5. Characterization of the Catalysts

XRD (X-ray diffraction, Smartlab (9)) analysis was also conducted to identify the main chemical phases in electrodes. The morphology and the element distribution of the Ni-Cu bimetallic catalyst were characterized by the methods of SEM (scanning electron microscope, Zeiss Gemini 300 SEM), and EDS (energy dispersive x-ray spectroscopy, Oxford Ultim MAX EDXS). The amounts of Ni and Cu in electrodes were roughly quantified with the results of EDS analysis in Fig. 10, for qualitative comparison on the performance of the electrode before and after usage with different Ni/Cu ratios. More accurate amounts of Ni and Cu in the electrode were quantified with the method of ICP-OES (Inductively Coupled Plasma Optical Emission Spectrometer, Thermo Scientific, Icap 6300) in Fig. 5 for optimization of the Ni/Cu ratio in electrode. Before analysis, the electrode was immersed into an acid solution (2 M HNO_3) in 50 °C for 1 hour, to transfer the metals from the surface of electrode into the aqueous solution. The solution was then diluted with deionized water, and the sample was used for analysis by ICP-OES.

RESULTS AND DISCUSSION

1. Characterization of Catalysts

The SEM and EDS images of the CalZIF, the CP with a coating layer of CalZIF (1 mg·cm^{-2}), and the Ni-Cu bimetallic catalyst with and without the mid-layer of CalZIF (1 mg·cm^{-2}) are shown in Fig. 1 and Fig. 2. It can be seen that the CalZIF particles are generally in a truncated cubic form and the sizes of the particles are uniform with an average diameter of 50 nm. A coarse and compact surface is formed, when CalZIF is coated on the surface of CP. After electrodeposition with Ni and Cu, there appear many half-spherical protuberances on the catalyst surface with the mid-layer of CalZIF, while the surface is smoother if there is no CalZIF

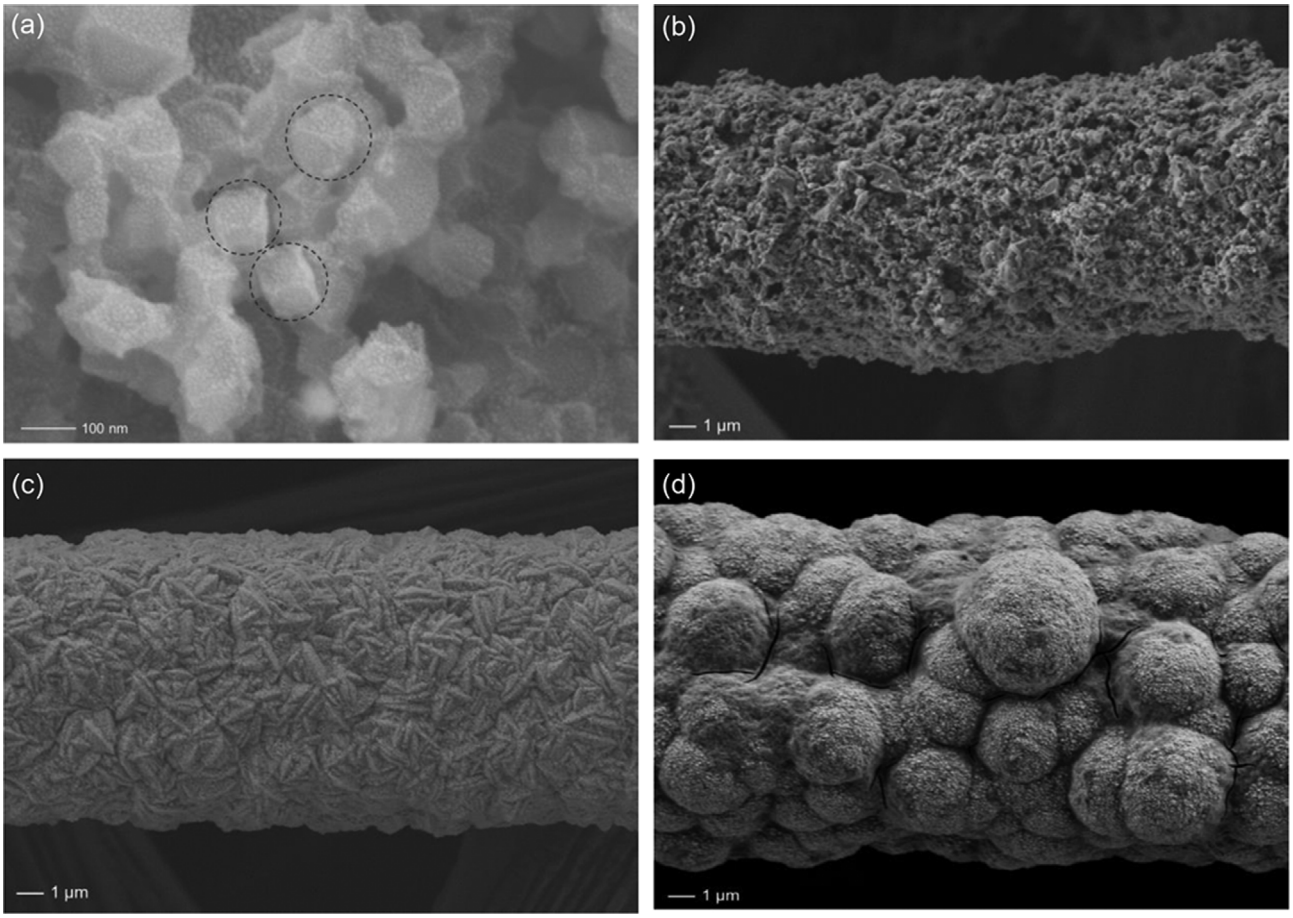

Fig. 1. SEM images of CalZIF (a), CP coated with a layer of CalZIF (b), NiCu/CP (c), NiCu/CalZIF/CP (d).

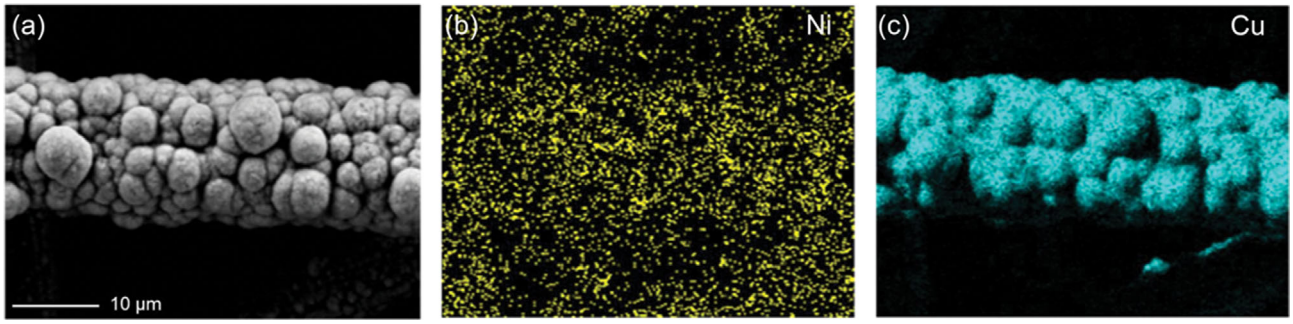

Fig. 2. EDS analysis of NiCu/CalZIF/CP (a), distribution of Ni in NiCu/CalZIF/CP (b), and distribution of Cu in NiCu/CalZIF/CP (c).

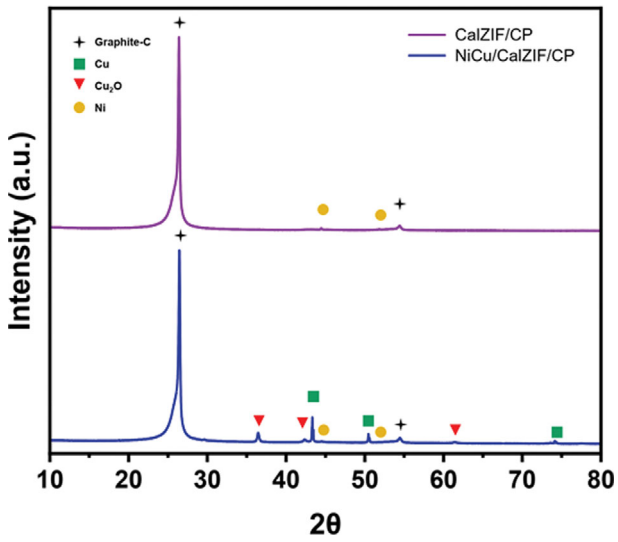

Fig. 3. XRD analysis on the catalysts before and after ED treatment, with and without the Ni-Cu bimetallic layer.

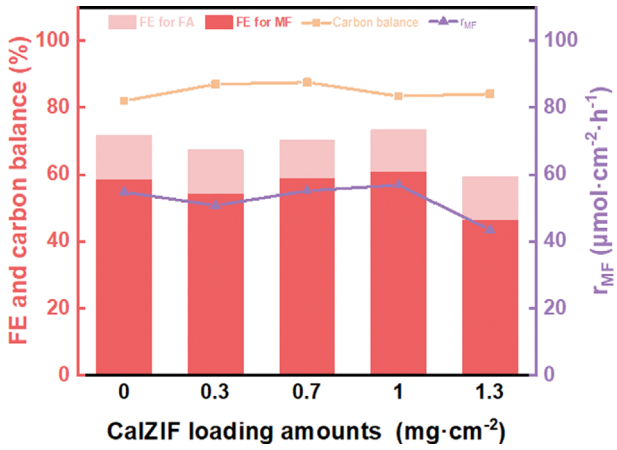

Fig. 4. FEs of products and PR of MF under the catalysis of NiCu/CalZIF/CP with different loading amounts of CalZIF.

between the metal layer and the CP substrate. It indicates that the scattered CalZIF particles may work as seeds and preferentially induce the depositions of Cu^{2+} and Ni^{2+} ions in electrolyte around the fine CalZIF particles, forming the ball like protuberances on the surface.

Seen from the distribution of elements, the surface is almost entirely covered by Cu atoms, and only a very little amount of Ni can be found. Herein, only a trace amount of Ni is loaded as a catalyst promoter, because it has been reported that Cu plays the base role in catalyzing the formation of MF from ECR of FF [22].

The XRD patterns in Fig. 3 show that a great deal of graphite C and a little of Ni are identified in the coating layer of CalZIF over CP (CalZIF/CP). By contrast, besides the much graphic C and the trace amount of Ni, the substances of Cu and Cu_2O are also found in the Ni-Cu bimetallic catalyst with the mid-layer of CalZIF (NiCu/CalZIF/CP). The weak signals of Ni in the two patterns are accordant with the low contents of Ni in the both samples, as the EDS characterization illustrated.

2. Influence of the Electrode Characteristics

The influence of the loading amount of CalZIF in the NiCu/CalZIF/CP electrode (metal layer amount of 3 mg·cm^{-2}) are investigated in the range of 0-1.3 mg·cm^2. The variations of the total FE of organic products (summary FE of MF and FA), the FE of MF, the FE of FA and the PR of MF are shown in Fig. 4. It can be seen that the FEs of organics and the PR of MF increase with the increasing dosage of CalZIF in the range from 0.3 mg·cm^2 to 1 mg·cm^2, and then decline rapidly after 1 mg·cm^2. For the electrode (NiCu/CP) without the mid-layer of CalZIF, the performance of the catalyst is slightly worse than the optimal case with 1 mg·cm^{-2} CalZIF. It means that a proper dosage of the CalZIF can improve the catalytic performance of the electrode, but in a slight degree under the present conditions. The regulation should be resulted from the compromise of two factors. On the one hand, there are more active sites on the electrode, due to the roughening of the surface resulted from the inducing deposition of metals on the surface of CalZIF. However, on the other hand, the space among CP fibers are filled with the CalZIF powders, which reduces the exposed area of the CP fibers, and thus decreases the number of active sites of metals.

The influence of the Ni/Cu mass ratio in the NiCu/CalZIF/CP electrode (metal layer amount of 3 mg·cm^{-2} and CalZIF amount of 1 mg·cm^{-2}) is investigated. Herein, three bimetallic catalysts with Ni/Cu mass ratios of 0.0003, 0.04, 0.41 (quantified with the method of ICP-OES, respectively obtained under ED potentials of −0.02 V, −0.12 V, −0.42 V, vs. RHE) are discussed, and compared with the electrode with mono Cu or mono Ni in the metal layer. The results are shown in Fig. 5. It can be seen that the total FE of organics, the

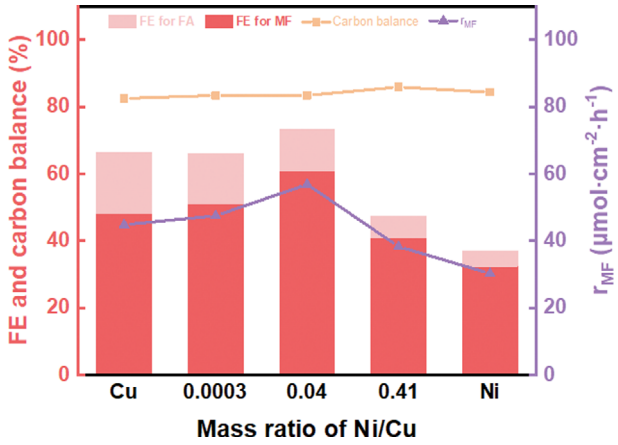

Fig. 5. FEs of products and PR of MF under the catalysis of NiCu/CalZIF/CP with different Ni/Cu mass ratios.

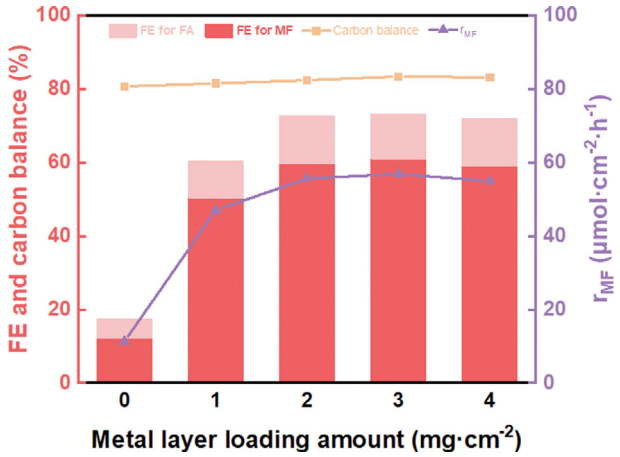

Fig. 6. FEs of products and PR of MF under the catalysis of NiCu/CalZIF/CP with different loading amount of metal layer.

FE of MF, and the PR of MF are highest at the optimal Ni/Cu ratio of 0.04. The phenomena may be attributed to the varied distributions of Ni and Cu sites on the electrode. The Ni and Cu distributions are influential to the synergistic effect of the two metals with different mechanic roles, as different atoms in FF molecule may simultaneously be adsorbed on different neighbouring metal sites. Specifically, the performance of the metal layer with mono Cu is more advantageous for the generation of organics but in a lower MF-to-FA ratio, while the mono Ni benefits the formation of H_2 with a higher selectivity of MF in organic products. Seen from the relation between the Ni/Cu ratio and the working potential, because the standard electric potential of Ni^{2+}/Ni^0 (–0.257 V) is significantly lower than that of Cu^{2+}/Cu (0.342 V), the Cu^{2+} ions in electrolyte are much easier to be reduced than the Ni^{2+} ions. It means that a lower working potential (higher potential absolute value) favors the deposition of Ni^{2+} more than that of Cu^{2+}. So, the Ni/Cu ratio remarkably increases with the decrease of working potential (the increase of potential absolute value). So, the Ni/Cu ratio (0.0003, 0.04, 0.41) remarkably increases with the decrease of working potential (the increase of potential absolute value, –0.02 V, –0.12 V, –0.42 V (vs. RHE)).

The influence of the loading amount of metal layer in the NiCu/CalZIF/CP electrode (Ni/Cu mass ratio of 0.04 and CalZIF amount of 1 mg·cm^{-2}) are investigated in the range of 0-4 mg·cm^{-2}. The loading amount of metal layer is controlled by adjusting the ED time in the range of 0-800 s. The results are shown in Fig. 6. It can be seen that the FEs of organics and the PR of MF increase with the increase of metal layer, and the variation is in fast rate before 1 mg·cm^{-2} and then becomes stable. Herein, the optimal loading amount of the metal layer is suggested to be 3 mg·cm^{-2}. For the electrode without metal layer (0 mg·cm^{-2}), the performance of the catalyst is remarkably worse. It means that the roles of the metal layer are essential and significant for the reaction, while the influence becomes insensitive in higher dosages. It is understandable, considering that the exposed active sites of metals cannot endlessly increase with the increase of metal dosage, due to the overlaps of metal atoms on the limited surface of support.

3. Influence of Current Density and Acidity

The influence of current density on the ECR of FF with the prior optimized NiCu/CalZIF/CP bimetallic catalyst (CalZIF amount of

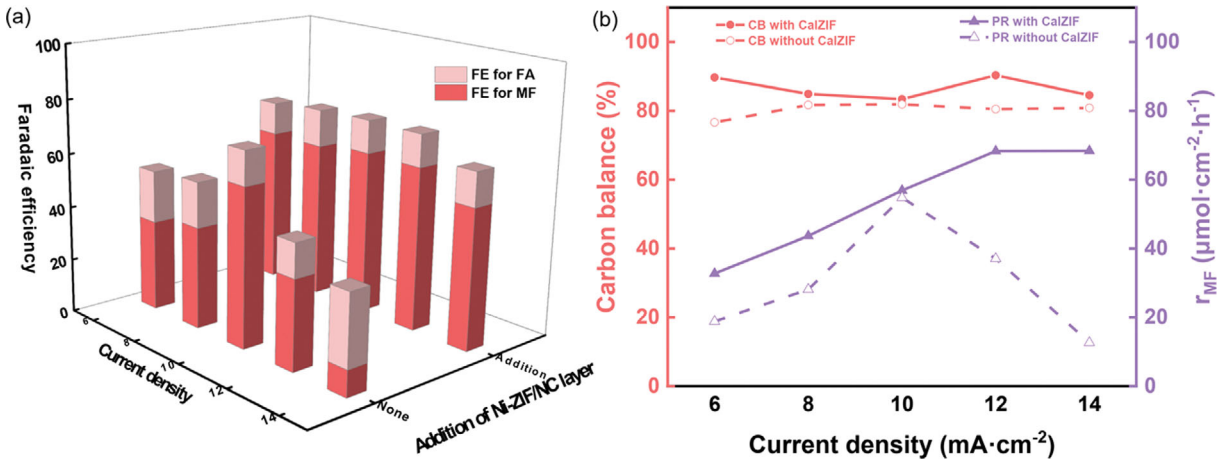

Fig. 7. FEs of products (a) and PR of MF (b) under the catalysis of NiCu/CalZIF/CP with different current densities.

1 mg·cm^{-2}, and metal layer amount of 3 mg·cm^{-2}) is investigated in the range of 6-14 mA·cm^{-2}. Comparative experiments are also conducted using the catalyst with a support of bare CP (NiCu/CP), to highlight the functions of the mid-layer of CalZIF. The results are illustrated in Fig. 7. It can be seen that for the system without CalZIF, the FEs of organics and the PR of MF increase with the increase of current density first and then decline after 10 mA·cm^{-2}. The maximum FE of MF (59%) and the largest PR of MF (55 μmol·cm^{-2}·h^{-1}) are obtained at the optimal current density of 10 mA·cm^{-2}. By contrast, for the system with CalZIF, the variation of FE illustrates a rising-first-and-declining-later trend with the increase of current density as well, while the maximum FE of MF (61%) and the largest PR of MF (68 μmol·cm^{-2}·h^{-1}) are even higher and appear at the current of 12 mA·cm^{-2}. Particularly, the FE variation degree is much slighter under the presence of CalZIF, and the PR variation of MF becomes stable after 12 mA·cm^{-2} instead of reducing, which is significantly different to that in the system without CalZIF. It indicates that in the system with CalZIF, the reaction is insensitive to the variation of current density, which is advantageous for improving the anti-interference of current in the reaction. The influence of current mainly lies in the following aspects. On the one hand, the increase of current is promotive to the conversion of FF, which leads to the increase of the FE of organics in lower current densities. On the other hand, when the supplying rate of electrons is beyond the electron consumption rate for conversion of FF, more electrons will be shared for generation of H2, and thus decreases the FE of organics at a high current density.

The influence of electrolyte acidity on the ECR of FF with the NiCu/CalZIF/CP bimetallic catalyst (CalZIF amount of 1 mg·cm^{-2}, and metal layer amount of 3 mg·cm^{-2}) is investigated at the optimal current density of 12 mA·cm^{-2}. The results under different H_2SO_4 concentrations in the range from 0.1 M to 0.6 M are illustrated in Fig. 8. It can be seen that the FEs of organics and the PR of MF increase with the increase of H_2SO_4 concentration before 0.2 M, and then decline slowly till 0.5 M, and finally reduce rapidly. As the Eqs. (1), (2) and (3) illustrated, H^+ is a reactant in each of the half-cell reactions, so the increase of H^+ concentration is promotive to all of the three reactions. However, the promoting degrees are different to different reactions, which is essentially determined by the competitions of the three reactions with different consumption rates of H^+ under different H^+ concentrations. As a compromise result, in the lower H_2SO_4 concentration range of 0.1-0.2 M, the increase of H^+ is more favorable to the generation of MF, as more H^+ is needed (stoichiometric coefficient of 4) therein. By contrast, in the range of 0.2-0.6 M with more H^+ ions in electrolyte than that of 0.1-0.2 M, the formation of H_2 by HER process is enhanced remarkably, which leads to the decrease of FEs of organics. At the highest H_2SO_4 concentration of 0.6 M, the total FE of organics even decreases to a level below 60%. In general, MF can be remarkably more generated than FA under an acidic condition, and the maximum values of the total FE of organics (82%), the FE of MF (66%), and the PR of MF (74 μmol·cm^{-2}·h^{-1}) are respectively obtained at the optimal H_2SO_4 concentration of 0.2 M.

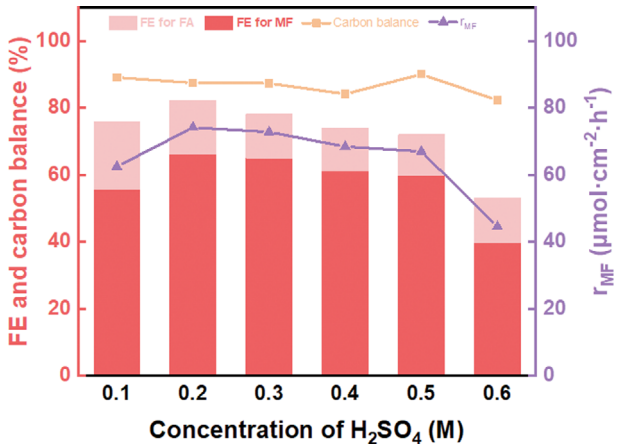

Fig. 8. FEs of organic products and PR of MF under the catalysis of NiCu/CalZIF/CP with different H_2SO_4 concentrations.

In general, the total FE of organics, the FE of MF, and the PR of MF, respectively reach to their maximum values of 82%, 66% and 74 μmol·cm^{-2}·h^{-1}, using the optimal NiCu/CalZIF/CP electrode, with CalZIF dosage of 1 mg·cm^{-2}, Ni/Cu ratio of 0.04, and metal layer amount of 3 mg·cm^{-2}, under the optimized ECR conditions of H_2SO_4 concentration of 0.2 M and current density of 12 mA·cm^{-2}. Compared with some representative literature work [2,4,22],

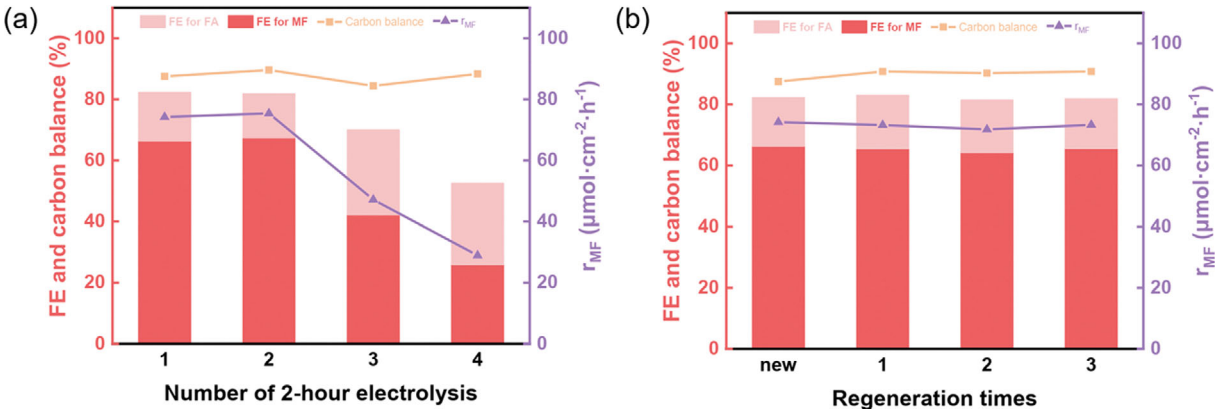

Fig. 9. FEs of organic products and PR of MF in 4 times of running (a) and 3 times of regeneration of the NiCu/CalZIF/CP electrode performance (b).

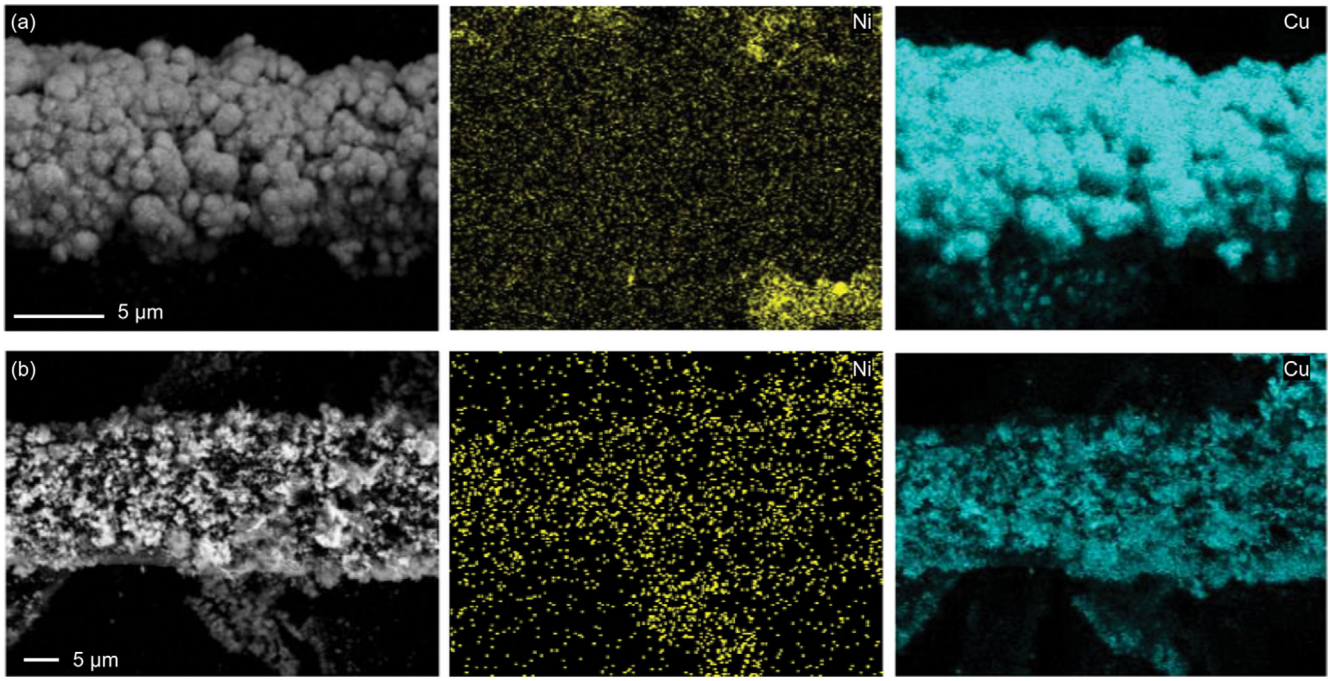

Fig. 10. EDS Images of the NiCu/CalZIF/CP electrodes after 4-hour reaction (a) and after 8-hour reaction (b).

the performances of different electrodes have different advantages, and we get a higher productivity of MF, but in a moderate level of the FE of MF.

4. Stability and Regenerability of the Electrode

Four times of experiments were conducted, to investigate the stability of the mentioned optimal electrode, under the optimized conditions. The results are illustrated in Fig. 9(a). It can be seen that the total FE of organics as well as the FE of MF remarkably reduces after 2 times of operations. It means that the stability of the electrode is less satisfactory, although the catalyst performs pretty good for preparation of MF from ECR of FF within 2 cycles of running.

The morphological characteristics of the electrodes after 4-hour reaction (equivalent to 2 cycles of running, and 2 hours for each run) and after 8-hour reaction were analyzed by SEM/EDS method. The images are shown in Fig. 10. It can be seen that compared with the initial morphology of the electrode before usage (Fig. 2(d)), the electrode after 4-hour reaction keeps in similar surface characteristics with many hemispheric protuberances, but in shorter radius, while the one after 8-hour reaction becomes very rough and loose. Seen from the Ni/Cu ratio (quantified with the method of EDS), the value is highest for the electrode before usage (0.05), and then it decreases with increasing time of reaction (0.035 after 4-hour reaction and 0.008 after 8-hour reactions). It indicates that the deactivation of catalyst is mainly caused by the loss and the agglomeration of the metal atoms, which are resulted from the corrosion and rearrangement of the metals over the surface of electrode. Comparatively, the corrosion of Ni is faster than that of Cu under the present conditions.

As a remedy method, the regenerability of the electrode is tested. The regeneration of the electrode is conducted via a two-step process. Firstly, the metal layer of the electrode is dissolved in the electrolyte (the same solution for electrodeposition of metal layer) through the method of anode electrolysis with a cathode of Pt wire, at the current of 13.3 $mA \cdot cm^{-2}$ for 600 seconds; then, the positions of anode and cathode are switched, to make the dissolved metal ions in electrolyte deposited on the CalZIF/CP support again at the same current of 13.3 $mA \cdot cm^{-2}$ for 600 seconds. As the SEM image in Fig. 11 showed, after regeneration, the electrode surface recovers back to rough and compact with many hemispheric protuberances again. The performances of the regenerated electrodes are shown in Fig. 10(b). It can be seen that after 3 times of regeneration, the CB value, the total FE of organics, the FE of MF, and the PR of MF are all similar to the level of the original electrode, which verifies the availability of the regeneration method and the regeneralbility of the electrode.

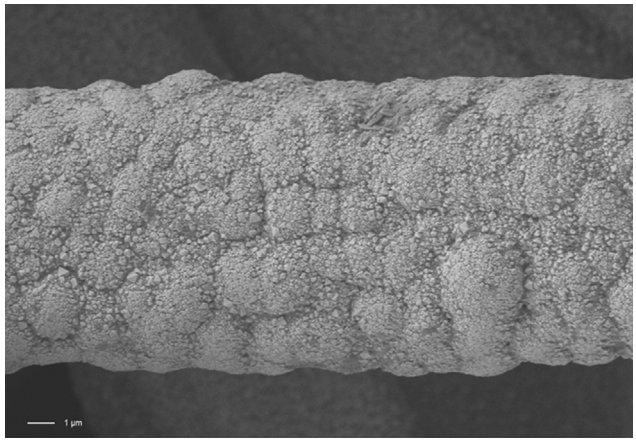

Fig. 11. SEM image of the NiCu/CalZIF/CP electrode after regeneration.

5. Mechanism Discussion

To investigate the reaction mechanism, the performances of the

Table 1. ECR performances of the electrodes in different compositions

Electrode	FE for MF (%)	FE for FA (%)	PR (μmol·cm^{-2}·h^{-1})	Carbon balance (%)
Bare CP	0	5	0	99
CalZIF/CP	12	5	11	81
Ni/CalZIF/CP	32	4	30	84
Cu/CalZIF/CP	48	18	45	82
NiCu/CalZIF/CP	61	12	57	83

Note: ECR conditions with current density of 10 mA·cm^{-2} and H_2SO_4 concentration of 0.5 M

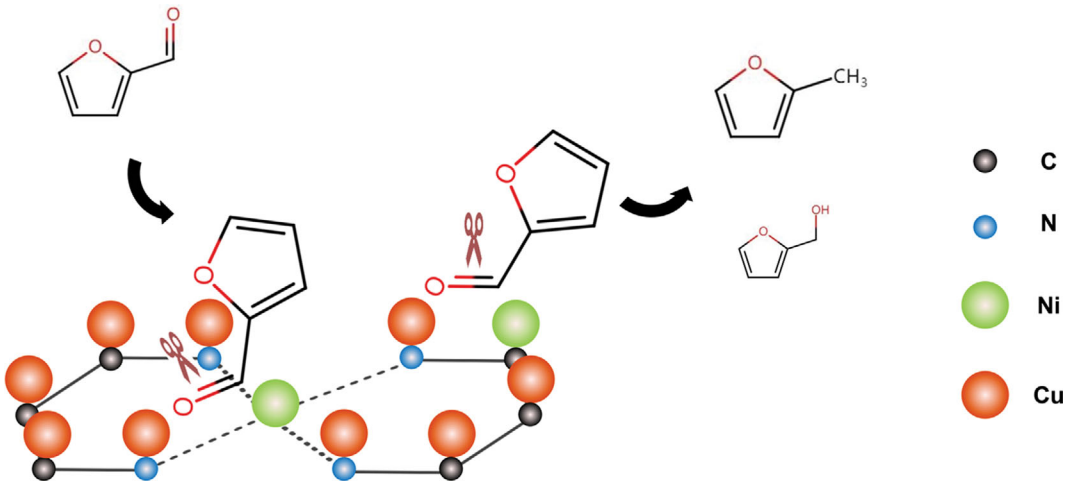

Scheme 2. Speculated reaction mechanism on the ECR of FF with the electrode of NiCu/CalZIF/CP.

electrodes in different compositions are compared, as shown in Table 1. It can be generalized that the bare CP nearly has no catalytic effect in promoting the formation of MF from ECR of FF; when CalZIF is coated on the surface of CP, the FEs of organics can be increased in comparison with the case of bare CP, but still remarkably lower than that with the bimetals of Ni and Cu; for the electrode with mono Ni or with mono Cu over the support of CalZIF/CP, the performance of the Ni is more advantageous for the generation of FA, while the one with mono Cu enhances the formation of MF more preferentially.

According to these regulations, it can be deduced that the catalytic role of the bimetallic composite electrode is mainly contributed from the bi-functions of the two metals. The bimetallic electrode with CalZIF has a better stability on anti-interference of current. It may be attributed to the coarse and compact surface of the NiCu/CalZIF/CP electrode with many half-spherical protuberances, which retards the corrosion of the metal layer. The role of Cu mainly lies in catalyzing the hydrogenation of the O atom in carbonyl group, while the Ni atom mainly promotes the hydrogenation of the carbonyl C atom, and the simultaneous adsorptions of C and O atoms of the carbonyl group on the two metals, weakens the carbonyl C-O bond, and thus favors the formation of MF. A schematic diagram of the reaction mechanism is speculated as shown in Scheme 2.

Kinetic analysis was conducted for analysis of the reaction route. The concentrations of FF, FA and MF varied with the going of reaction are recorded. The experiments are conducted using the mentioned optimal catalyst, under the optimized conditions. The

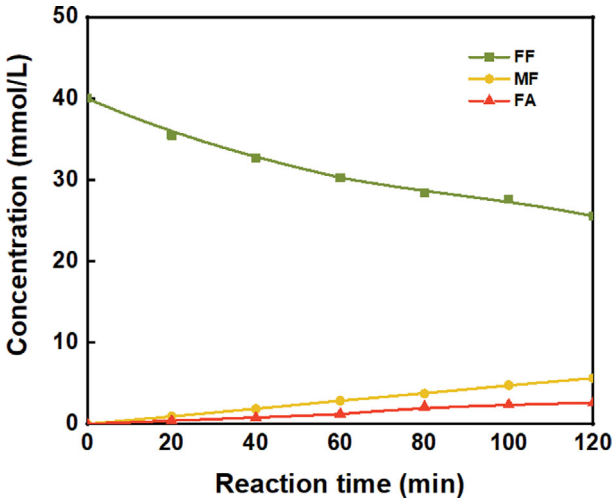

Fig. 12. Concentrations of FF, FA and MF in electrolyte varied with the proceeding of reaction.

results are illustrated in Fig. 12. It can be seen that both of FA and MF monotonously increase with the increase of reaction time. It indicates that MF is parallelly generated along with FA, rather than through a consecutive route via an intermediate product of FA, as there is no increasing period in the variation trend of FA. The conclusion is accordant with the literature result with different electrode or electrolyte [28,29].

Based on the time-dependent data, a kinetic model is further built by model fitting method. It is found that the data can well be fitted with a zero-order reaction model (R^2 for r_{MF} is 0.99, R^2 for r_{FA} is 0.98), which can be expressed by Eqs. (10)-(11):

$$r_{MF}=4.71\times10^{-5}\ mol\cdot L^{-1}\cdot min^{-1} \quad (10)$$

$$r_{FA}=2.33\times10^{-5}\ mol\cdot L^{-1}\cdot min^{-1} \quad (11)$$

CONCLUSIONS

The electrocatalytic reduction (ECR) of furfural (FF) for synthesis of 2-methylfuran (MF) is investigated, using a sandwich-structured electrode (NiCu/CalZIF/CP), with an inner substrate of carbon paper (CP), a surface layer of Ni-Cu bimetallic catalyst (metal layer), and a middle layer of calcined Ni-ZIF-8 (CalZIF) particles. The formation of MF can be promoted under a proper loading amount of CalZIF in electrode. The production rate (PR) of MF increases with increasing current density first and then becomes stable, which is different to the reducing trend under higher current conditions in the system without CalZIF. Under the optimized ECR conditions with H_2SO_4 concentration of 0.2 mol/L and current density of 12 $mA\cdot cm^{-2}$, the total Faradaic efficiency (FE) of organics, the FE of MF, and the PR of MF, respectively reach to their maximum values of 82%, 66% and 74 $\mu mol\cdot cm^{-2}\cdot h^{-1}$, using the optimal NiCu/CalZIF/CP electrode, with Ni/Cu ratio of 0.04, metal layer amount of 3 $mg\cdot cm^{-2}$, and CalZIF dosage of 1 $mg\cdot cm^{-2}$. The catalytic role of the composite electrode is mainly attributed to the bi-functions of the two metals of Ni and Cu. The presence of CalZIF improves the stability of the electrode on anti-interference of current, possibly attributed to the coarse and compact surface with many half-spherical protuberances, retarding the corrosion of metal layer. The NiCu/CalZIF/CP electrode performs pretty good for preparation of MF within 4 hours' reaction, and then becomes worse. As a remedy method, the electrode can be regenerated after re-elctrodeposition. The deactivation of catalyst is related with the loss and the agglomeration of metal atoms, resulted from the corrosion and rearrangement of the metals over the surface of electrode.

ACKNOWLEDGEMENTS

We acknowledge the financial support by the National Key R&D Program of China (2019YFC1906700).

NOMENCLATURE

Abbreviations

CalZIF : calcined Ni-ZIF-8
CB : carbon balance
CP : carbon paper
DMF : N, N-dimethylformamide
EA : ethyl acetate
ECR : electrocatalytic reduction
ED : electrodeposition
FA : furfuryl alcohol
FE : faradaic efficiency
FF : furfural
HER : hydrogen evolution reaction
MF : 2-methylfuran
MOF : metal-organic framework
PR : production rate
WE : working electrode

CONFLICT OF INTEREST

There is no conflict of interest in the work

REFERENCES

1. C. Xu, E. Paone, D. Rodríguez-Padrón, R. Luque and F. Mauriello, *Chem. Soc. Rev.*, **49**(13), 4273 (2020).
2. S. Chen, R. Wojcieszak, F. Dumeignil, E. Marceau and S. Royer, *Chem. Rev.*, **118**(22), 11023 (2018).
3. S. Bhogeswararao and D. Srinivas, *J. Catal.*, **327**, 65 (2015).
4. A. Bohre, S. Dutta, B. Saha and M. M. Abu-Omar, *ACS Sustain. Chem. Eng.*, **3**(7), 1263 (2015).
5. S. Shiva Kumar and H. Lim, *Energy Rep.*, **8**, 13793 (2022).
6. L. Wang, Y. Zhu, Z. Zeng, C. Lin, M. Giroux, L. Jiang, Y. Han, J. Greeley, C. Wang and J. Jin, *Nano Energy*, **31**, 456 (2017).
7. H. Kim, H. Park, H. Bang and S.-K. Kim, *Korean J. Chem. Eng.*, **37**(8), 1275 (2020).
8. R. M. Al Radadi and M. A. M. Ibrahim, *Korean J. Chem. Eng.*, **38**(1), 152 (2021).
9. Y. Lei, Z. Wang, A. Bao, X. Tang, X. Huang, H. Yi, S. Zhao, T. Sun, J. Wang and F. Gao, *Chem. Eng. J.*, **453**, 139663 (2023).
10. X. An, S. Li, X. Hao, Z. Xie, X. Du, Z. Wang, X. Hao, A. Abudula and G. Guan, *Renew. Sust. Energ. Rev.*, **143**, 110952 (2021).
11. W. J. Wang, L. Scudiero and S. Ha, *Korean J. Chem. Eng.*, **39**(3), 461 (2022).
12. F. Rehman, M. Delowar Hossain, A. Tyagi, D. Lu, B. Yuan and Z. Luo, *Mater. Today*, **44**, 136 (2021).
13. S. H. Jeon, K. Kim, H. Cho, H. C. Yoon and J.-I. Han, *Korean J. Chem. Eng.*, **38**(6), 1272 (2021).
14. X. Lu, J. Wang, W. Peng, N. Li, L. Liang, Z. Cheng, B. Yan, G. Yang and G. Chen, *Fuel*, **331**, 125845 (2023).
15. Y. Du, X. Chen and C. Liang, *Mol. Catal.*, **535**, 112831 (2023).
16. U. Sanyal, K. Koh, L. C. Meyer, A. Karkamkar and O. Y. Gutiérrez, *J. Appl. Electrochem.*, **51**(1), 27 (2021).
17. P. Zhou, L. Li, V. S. S. Mosali, Y. Chen, P. Luan, Q. Gu, D. R. Turner, L. Huang and J. Zhang, *Angew. Chem. Int. Ed.*, **61**(13), e202117809 (2022).
18. S. Jung and E. J. Biddinger, *ACS Sustain. Chem. Eng.*, **4**(12), 6500 (2016).
19. Z. Yang, X. Chou, H. Kan, Z. Xiao and Y. Ding, *ACS Sustain. Chem. Eng.*, **10**(22), 7418 (2022).
20. S. Jung and E. J. Biddinger, *Energy Technol.*, **6**(7), 1370 (2018).
21. S. Jung, A. N. Karaiskakis and E. J. Biddinger, *Catal. Today*, **323**, 26 (2019).
22. P. Zhou, Y. Chen, P. Luan, X. Zhang, Z. Yuan, S.-X. Guo, Q. Gu, B. Johannessen, M. Mollah, A. L. Chaffee, D. R. Turner and J. Zhang, *Green Chem.*, **23**(8), 3028 (2021).
23. P. Nilges and U. Schröder, *Energy Environ. Sci.*, **6**(10), 2925 (2013).
24. A. S. May and E. J. Biddinger, *ACS Catal.*, **10**(5), 3212 (2020).

25. X. H. Chadderdon, D. J. Chadderdon, J. E. Matthiesen, Y. Qiu, J. M. Carraher, J.-P. Tessonnier and W. Li, *J. Am. Chem. Soc.*, **139**(40), 14120 (2017).
26. R. J. Dixit, K. Bhattacharyya, V. K. Ramani and S. Basu, *Green Chem.*, **23**(11), 4201 (2021).
27. X. Lan, N. Huang, J. Wang and T. Wang, *ChemComm*, **54**(6), 584 (2018).
28. A. S. May, S. M. Watt and E. J. Biddinger, *React. Chem. Eng.*, **6**(11), 2075 (2021).
29. N. Shan, M. K. Hanchett and B. Liu, *J. Phys. Chem. C*, **121**(46), 25768 (2017).